(Preprint) AAS 11-635

# A MINIMUM $\triangle$V ORBIT MAINTENANCE STRATEGY FOR LOW-ALTITUDE MISSIONS USING BURN PARAMETER OPTIMIZATION

**Aaron J. Brown***

Orbit maintenance is the series of burns performed during a mission to ensure the orbit satisfies mission constraints. Low-altitude missions often require non-trivial orbit maintenance $\Delta$V due to sizable orbital perturbations and minimum altitude thresholds. A strategy is presented for minimizing this $\Delta$V using impulsive burn parameter optimization. An initial estimate for the burn parameters is generated by considering a feasible solution to the orbit maintenance problem. An low-lunar orbit example demonstrates the $\Delta$V savings from the feasible solution to the optimal solution. The strategy's extensibility to more complex missions is discussed, as well as the limitations of its use.

## INTRODUCTION

"Orbit maintenance," as discussed in this paper, refers to the series of burns that must be performed during a mission to ensure the vehicle's orbit satisfies all mission constraints. An orbit maintenance strategy is often devised pre-mission to meet these constraints and dictate exactly what burns are needed. The problem of determining an appropriate orbit maintenance strategy is certainly not new, as almost any mission orbiting close to its central body has grappled with this question. Such missions include the International Space Station (formerly Space Station Freedom),[1] TOPEX/Poseidon,[2] the Lunar Reconnaissance Orbiter (LRO),[3] and the Mars Reconnaissance Orbiter (MRO).[4]

Low-altitude missions in particular often require non-trivial orbit maintenance $\Delta$V due to sizable orbital perturbations and their proximities to minimum altitude thresholds. These perturbations come from non-spherical mass distributions in the central body, third-body effects, and atmospheric drag (when applicable). Minimizing the $\Delta$V spent on orbit maintenance while meeting mission constraints is clearly desirable for mission planning purposes. This paper presents a strategy for accomplishing these goals using impulsive burn parameter optimization.

Like the orbit maintenance problem, trajectory optimization problems such as minimum fuel or minimum time orbit transfers are not new, and have been solved for decades using parameter optimization. This study aims to bring the realms of orbit maintenance and parameter optimization together in an effort to generate an optimal solution to the orbit maintenance problem. While this approach can be taken for any mission in orbit about its central body, this paper will focus on low-altitude missions because of their potentially high orbit maintenance costs.

*Aerospace Engineer, Flight Dynamics Division, NASA Johnson Space Center, Mail Code DM34, 2101 NASA Parkway, Houston, TX 77058.

A low-lunar orbit example with simple mission constraints is used to demonstrate the strategy's effectiveness. In principle, this strategy is extensible to missions such as LRO that have more complex mission constraints. In the following sections, vectors are denoted in **bold** and scalars in *italics*.

## ASSUMPTIONS AND EQUATIONS OF MOTION

For this analysis, a low-altitude mission is assumed in which the initial orbit conditions of the vehicle are specified. The mission constraints under consideration include final orbit conditions (i.e. endpoint equality constraints), and a constant minimum altitude threshold (i.e. a path inequality constraint). Figure 1 provides an abstract representation of the mission.

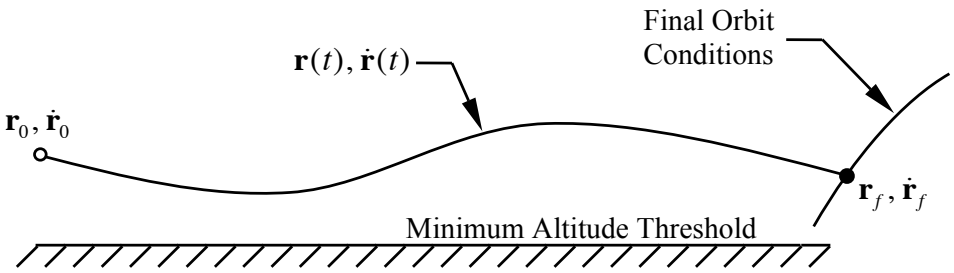


**Figure 1. Abstract Representation of a Low-Altitude Mission**

The equations of motion are

$$\ddot{\mathbf{r}} = -\frac{\mu}{r^3}\mathbf{r} + \mathbf{f} \tag{1}$$

where $\mathbf{r}$ is the position, $\mu$ is the gravitational constant, and $\mathbf{f} = \mathbf{f}(\mathbf{r}, \dot{\mathbf{r}}, t)$ is the perturbing acceleration on the vehicle.

## DEFINING BURN PARAMETERS AND GENERATING INITIAL ESTIMATES

For low-altitude missions constrained only by a minimum altitude threshold, a standard orbit maintenance strategy (henceforth called the "standard strategy") can be applied in order to both define the burn parameters to be optimized and to generate their initial estimates. If the vehicle's orbit is perturbed by non-spherical gravity, drag, or some other force, it's periapse will tend to decrease over time. Depending on the vehicle's initial conditions and the minimum altitude threshold, the periapse may violate this threshold (and the vehicle may even impact the surface) before possibly trending positive (say, in the case of non-spherical gravity). In the standard strategy, when the next periapse is predicted to drop below the minimum altitude threshold, an impulsive, horizontal burn is performed at the apoapse immediately prior in order to raise periapse back to a specified reference altitude. This procedure is repeated as necessary over the course of the mission. Each time the next periapse is predicted to violate the minimum altitude threshold, periapse is boosted to the reference altitude. This periapse-raising "phase" constitutes Part I of the standard strategy.

In general, the final state at the end of the periapse-raising phase will not meet the final orbit conditions. In Part II of the standard strategy, a minimum-$\Delta$V two-burn impulsive transfer is performed to meet these constraints. This transfer is accomplished by solving a separate parameter

optimization sub-problem in which the parameters are the times of ignition (TIGs) and $\Delta$V components ($\Delta V_x$, $\Delta V_y$, $\Delta V_z$) of the two impulses, along with the transfer time between the initial and final orbits. The "initial" orbit for this sub-problem is given by the final state at the end of the periapse-raising phase, and the "final" orbit is defined by the final orbit conditions. The transfer orbit is constrained to depart from the "initial" orbit any time after the end of the periapse-raising phase. Ocampo[5] provides several approaches to solving this sub-problem. In summary, the process of raising periapse to the reference altitude (Part I) followed by a final two-burn orbit transfer (Part II) constitute the standard strategy.

Following the optimized two-burn transfer, the TIGs and $\Delta$V components of all impulsive burns performed in the standard strategy become the parameters ($\mathbf{X}$) for a larger burn optimization problem. The parameter values resulting from the standard strategy are used for the initial estimates ($\mathbf{X}_0$). The standard strategy also provides a baseline value of the objective function, which is the sum of the impulsive $\Delta$V magnitudes throughout the mission. Qualitatively then, the objective function tells us how much $\Delta$V was required to "fly" a given strategy, i.e. to maintain the orbit and not violate any mission constraints.

To illustrate the standard strategy, consider a hypothetical spacecraft in a low-altitude orbit around the Moon. The vehicle starts in a 100 km altitude, circular, polar orbit, and must return to those same conditions after completing a 60-day mission. These conditions are listed in Table 1 and constitute the first case study (Case 1). A variation on these conditions will be examined later in Case 2. During the mission, the vehicle must stay above a minimum altitude threshold of 80 km.

A realistic application of the Case 1 conditions would be a crewed mission to the Moon to examine a polar landing site.[6] The vehicle would stay in a low-altitude orbit while a surface module would land at the site and commence extended surface operations. The vehicle is required to stay in a low-altitude orbit in order to support surface aborts (if necessary) but also must stay above the minimum altitude threshold. At the conclusion of surface operations, the vehicle would perform a two-burn orbit transfer to prepare for ascent and rendezvous of the surface module.

**Table 1. Low Lunar Orbit Initial and Final Conditions - Case 1**

| Element | Initial Condition | Final Condition |
|---|---|---|
| $h$ (km) | 100 | 100 |
| $e$ | 0 | 0 |
| $i$ (deg) | 90 | 90 |
| $\Omega$ (deg) | 0 | – |
| $\omega$ (deg) | 0 | – |
| $\nu$ (deg) | 0 | – |

The only orbital perturbation considered in this study is non-spherical lunar gravity, modeled using LP150Q truncated to degree and order 8. The equations of motion are propagated using an Encke formulation and a modified Nyström numerical integrator.[7] During propagation, semi-major axis altitude, periapse altitude, apoapse altitude, eccentricity, and inclination are sampled at each periapse (i.e. $\nu = 0$) and are plotted in Figures 2 through 4. Note in Figures 2 and 3 that the effects of the two interior periapse-raising burns are clearly visible at approximately 28 and 55 days, respectively. As expected however, these effects are not visible in Figure 4 since these two burns are not designed to change inclination.

The standard strategy presents a very feasible solution to this orbit maintenance problem. More-

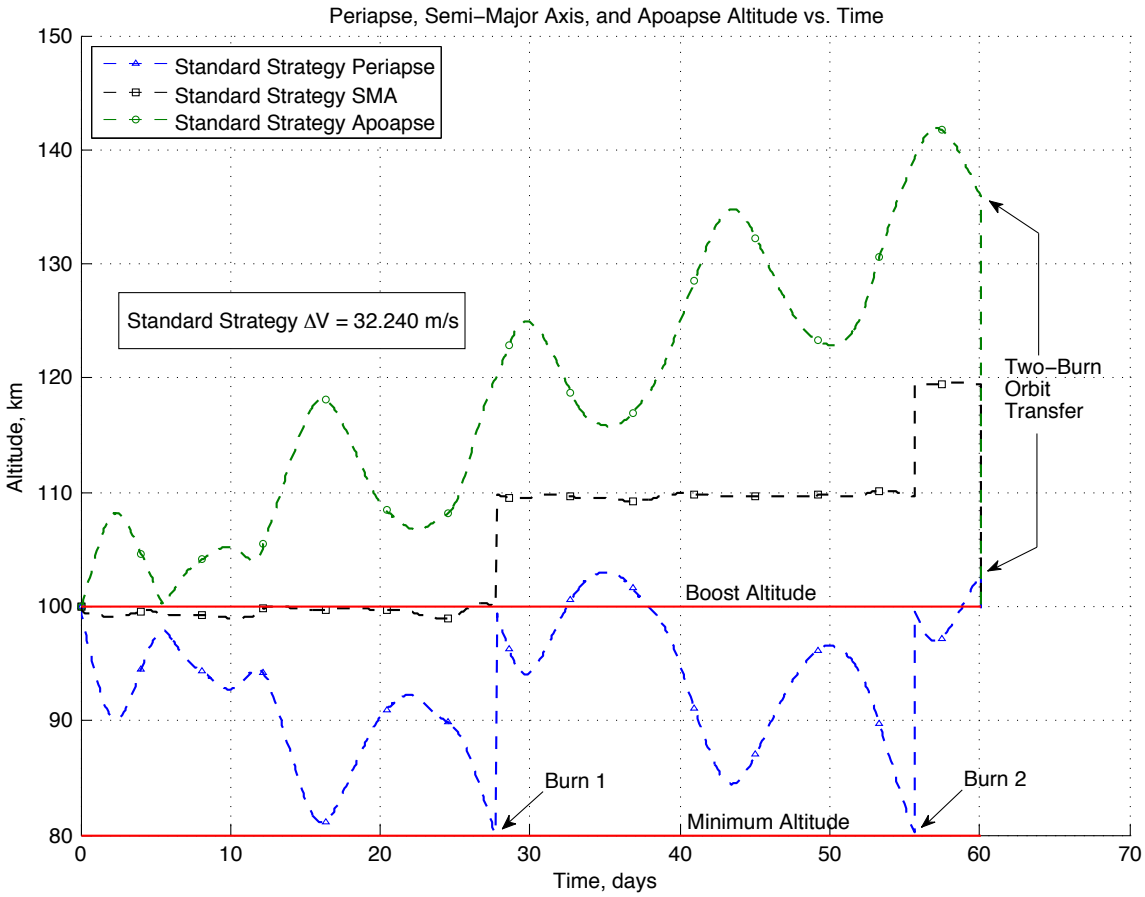


**Figure 2. Periapse, Semi-Major Axis, and Apoapse Altitude vs. Time Using Standard Strategy - Case 1**

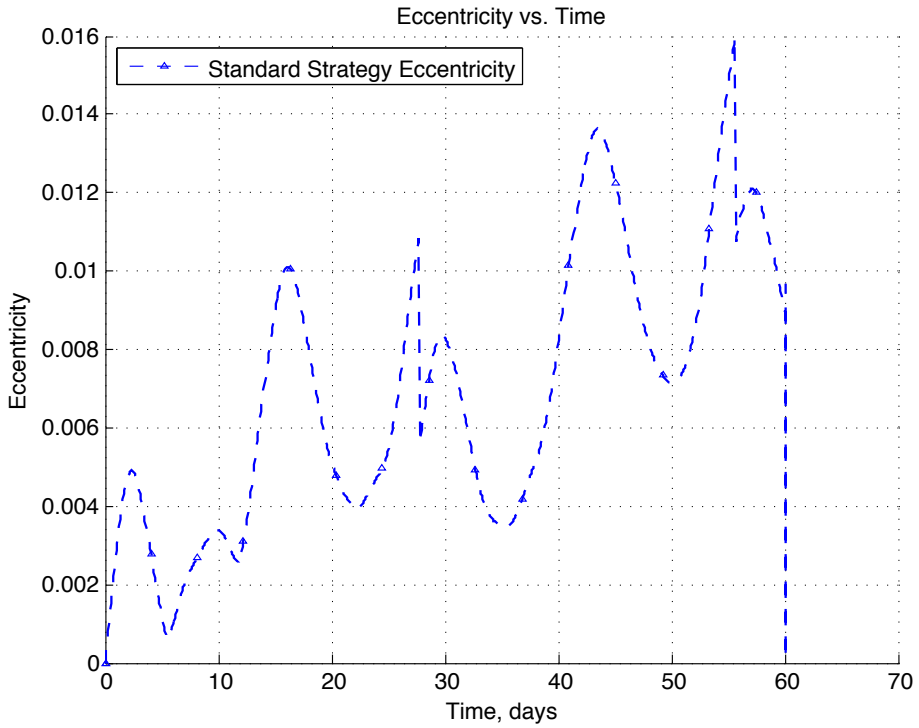


**Figure 3. Eccentricity vs. Time Using Standard Strategy - Case 1**

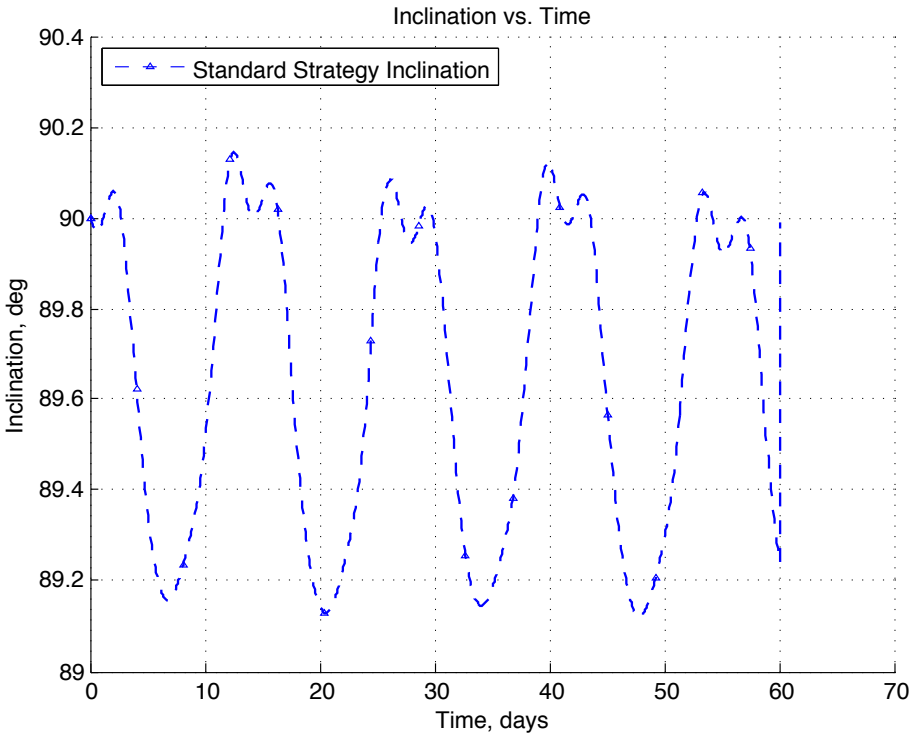


**Figure 4. Inclination vs. Time Using Standard Strategy - Case 1**

over, the solution seems not only feasible, but potentially optimal on its own. Each periapse-raising burn is performed horizontally and at apoapse, which minimizes the $\Delta$V needed to raise periapse back to the reference altitude. Additionally, the final two-burn transfer has been optimized to provide at least a locally minimal $\Delta$V solution. Summing these $\Delta$V magnitudes together would seemingly provide a minimum or near-minimum orbit maintenance $\Delta$V cost over the entire mission.

Further analysis, however, demonstrates that the orbit maintenance $\Delta$V can be reduced by solving a larger optimization problem that optimizes all burns simultaneously using the standard strategy as a starting point, rather than burn-by-burn using the standard strategy alone.

## PROBLEM STATEMENT

The larger optimization problem to be solved can be stated as follows. Minimize

$$J(\mathbf{X}) = \sum_{k=1}^{N} \Delta \mathrm{V}_k \tag{2}$$

subject to

$$\mathbf{c}_{eq}(\mathbf{r}_f, \dot{\mathbf{r}}_f) = \mathbf{0} \tag{3}$$

$$h(t) \geq h_{\min} \tag{4}$$

The equations of motion are given in Eq. (1), and $t_0$, $t_f$, $\mathbf{r}_0$, $\dot{\mathbf{r}}_0$ are specified. In Eq. (2), $N$ is the number of impulsive burns as determined by the standard strategy. As mentioned previously, this problem can be parameterized using the TIGs and $\Delta$V components of these burns. The parameter vector $\mathbf{X}$ is therefore

$$\mathbf{X} = \begin{pmatrix} t_1 & \Delta\mathbf{V}_1 & t_2 & \Delta\mathbf{V}_2 & \cdots & t_N & \Delta\mathbf{V}_N \end{pmatrix}^{\mathrm{T}}. \tag{5}$$

Note in Eq. (5) that $\Delta\mathbf{V}_1, \ldots, \Delta\mathbf{V}_N$ are **vectors** and not scalars. $\mathbf{c}_{eq}$ in Eq. (3) are the final orbit conditions (i.e. endpoint equality constraints). These can include final orbital elements to be targeted or other functions of the final position and velocity. Eq. (4) is the path inequality constraint for the constant minimum altitude threshold, $h_{\min}$.

To work within the context of a parameter optimization problem, the path inequality constraint is converted to an interior point inequality constraint that is imposed at the periapse preceding each burn. Recall that in the standard strategy, an impulsive burn is only executed when the altitude of the next periapse is predicted to drop below the minimum altitude threshold. Therefore in the standard strategy, the altitude of the periapse preceding the burn will represent the lowest altitude point along the path, since this was the point just prior to the violation (had no burn been performed). If the inequality constraint is met at each such point, then in general it will be met along the entire path.* Thus Eq. (4) is equivalent to

*Isolated points may exist along the trajectory in which periapse comes very close to, but does not violate the minimum altitude threshold. In these cases, the standard strategy dictates that no burn is performed since the threshold was not violated. In the subsequent optimization, however, the components of one or more burns preceding these points may change, and ultimately cause these points to now violate the threshold. No inequality constraints however will exist at these points to protect against this violation, since there were no burns in the standard strategy to "trigger" these

$$\mathbf{c}_{ineq} = \begin{pmatrix} h_{\text{min}} - h_{p_1} \\ h_{\text{min}} - h_{p_2} \\ \vdots \\ h_{\text{min}} - h_{p_N} \end{pmatrix} \leq \mathbf{0} \tag{6}$$

where $h_{p_k}$ is the altitude of the periapse preceding burn $k$.

Since $J$ is an explicit function of $\mathbf{X}$, the gradient of J is straightforward.

$$\left(\frac{\partial J}{\partial \mathbf{X}}\right)^{\mathrm{T}} = \begin{pmatrix} 0 & \frac{\Delta \mathbf{V}_1^{\mathrm{T}}}{\Delta \mathrm{V}_1} & 0 & \frac{\Delta \mathbf{V}_2^{\mathrm{T}}}{\Delta \mathrm{V}_2} & \cdots & 0 & \frac{\Delta \mathbf{V}_N^{\mathrm{T}}}{\Delta \mathrm{V}_N} \end{pmatrix}^{\mathrm{T}}. \tag{7}$$

If $\Delta \mathrm{V}_k = 0$, then the gradient is simply 0 for burn $k$. In contrast to $J$, the gradient of $\mathbf{c}$ (i.e. $(\partial \mathbf{c}/\partial \mathbf{X})^{\mathrm{T}}$), where $\mathbf{c} = \begin{pmatrix} \mathbf{c}_{eq}^{\mathrm{T}} & \mathbf{c}_{ineq}^{\mathrm{T}} \end{pmatrix}^{\mathrm{T}}$, is not an explicit function of $\mathbf{X}$ and must be approximated using finite differences or other comparable method.

Finally, suitable scale factors $\boldsymbol{S}$ are chosen for $\mathbf{X}$, $J$, and $\mathbf{c}$ to aid convergence in the optimization process. For each element *i* of $\mathbf{X}$, for *J*, and for each element *j* of $\mathbf{c}$, define

$$\mathrm{X}_{i_{scl}} = \frac{\mathrm{X}_i}{S_{\mathrm{X}_i}}, \quad J_{scl} = \frac{J}{S_J}, \quad \mathrm{c}_{j_{scl}} = \frac{\mathrm{c}_j}{S_{\mathrm{c}_j}} \tag{8}$$

so that $\mathbf{X}_{scl}$, $J_{scl}$, and $\mathbf{c}_{scl}$ become the "scaled" versions of $\mathbf{X}$, $J$, and $\mathbf{c}$, respectively. $\boldsymbol{S}_{\mathbf{X}}$, $S_J$, and $\boldsymbol{S}_{\mathbf{c}}$ are then chosen so that each scaled gradient

$$\frac{\partial J_{scl}}{\partial \mathrm{X}_{i_{scl}}} = \frac{\partial J}{\partial \mathrm{X}_i} \frac{S_{\mathrm{X}_i}}{S_J}, \quad \frac{\partial \mathrm{c}_{j_{scl}}}{\partial \mathrm{X}_{i_{scl}}} = \frac{\partial \mathrm{c}_j}{\partial \mathrm{X}_i} \frac{S_{\mathrm{X}_i}}{S_{\mathrm{c}_j}} \tag{9}$$

when evaluated at $t_0$ has an order of magnitude as close to $\pm 1$ as possible. This ensures that changes in $J$ and $\mathbf{c}$ will not be too steep (i.e. sensitive) nor too shallow (i.e. insensitive) as the optimizer varies $\mathbf{X}$.

## SOLUTION AND RESULTS

The optimization problem is solved using a sequential quadratic programming (SQP) algorithm implemented in MATLAB's *fmincon* function. The implementation is based on Chapter 18 of Nocedal and Wright.[8] At the solution point, *fmincon* returns the final parameter estimates, $\mathbf{X}_f$. Evidence that the solution is in fact a local minimum can be found in Figure 5, which plots the objective function history for Case 1.

Further evidence can be obtained by examining the first differential necessary conditions for a minimum. Let $\boldsymbol{\nu}_{eq}$ and $\boldsymbol{\nu}_{ineq}$ be the vectors of Lagrange multipliers associated with the equality and inequality constraints, respectively. An auxiliary Lagrangian function is then given by

$$L(\mathbf{X}, \boldsymbol{\nu}) = J(\mathbf{X}) + \boldsymbol{\nu}_{eq}^T \mathbf{c}_{eq} + \boldsymbol{\nu}_{ineq}^T \mathbf{c}_{ineq}. \tag{10}$$

constraints. To work around these isolated cases, it is sufficient to note where they exist in the standard strategy, and then to generate the optimal solution. If any of these points (that did not violate the threshold in the standard strategy) now violate the threshold in the optimal solution, inequality constraints can be manually added to $\mathbf{c}_{ineq}$ and the optimal solution can be re-generated. In the new solution, these points will no longer violate the minimum altitude threshold.

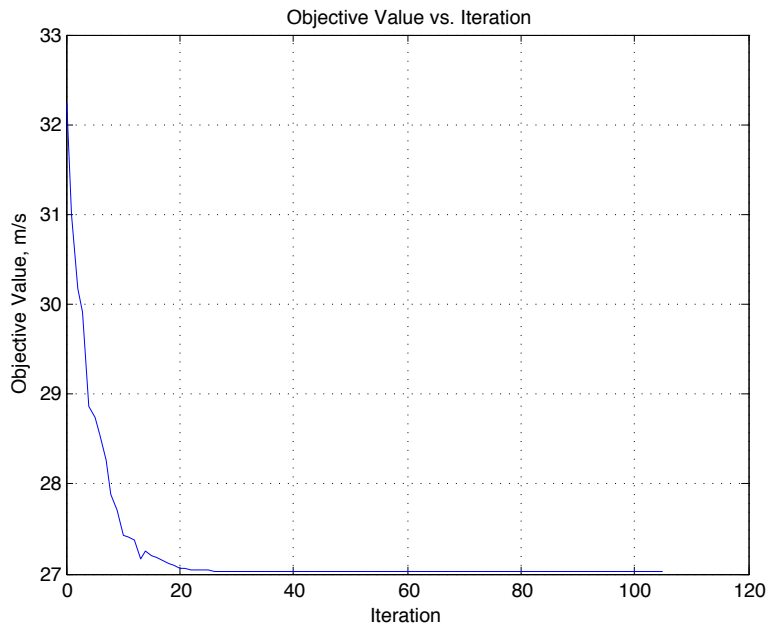


**Figure 5. Objective Value vs. Iteration - Case 1**

With this definition, the first differential necessary conditions for a minimum are

$$\left(\frac{\partial L}{\partial \mathbf{X}}\right)^{\mathrm{T}} = \mathbf{0} \tag{11}$$

$$\mathbf{c}_{eq} = \mathbf{0} \tag{12}$$

$$\mathbf{c}_{ineq} \leq \mathbf{0} \tag{13}$$

$$\boldsymbol{\nu}_{ineq} \geq \mathbf{0} \tag{14}$$

Though not shown here, these conditions are met to within the algorithm's tolerances at the solution point.

The initial and final parameter estimates ($\mathbf{X}_0$ and $\mathbf{X}_f$) and $\Delta$V magnitudes for the periapse-raising burns and the final orbit transfer burns for Case 1 are given in Tables 2 and 3. In these tables, the $\Delta$V components are expressed in a Local Vertical Local Horizontal (LVLH) coordinate system in which the Y axis points opposite the angular momentum vector, the Z axis points nadir, and the X axis completes the right-handed system. Semi-major axis altitude, periapse altitude, apoapse altitude, eccentricity, and inclination using both the standard strategy and parameter optimization for Case 1 are plotted in Figures 6 through 8. As shown in Figure 6, using parameter optimization with the standard strategy as a starting point reduces the orbit maintenance $\Delta$V in Case 1 from 32.240 m/s to 27.028 m/s, reflecting a **16%** savings over using the standard strategy alone.

The data suggest that the optimizer realized these savings through three primary adjustments.

1. Out-of-plane $\Delta$V (i.e. $\Delta V_y$) was added to Burns 1 and 2 in order to adjust the inclination downstream and reduce the out-of-plane $\Delta$V required in Burn 4.

2. Burn 3 was almost completed eliminated.

3. $\Delta V_x$ was subtracted from Burn 2. This adjusted the periapse altitude downstream such that no periapse correction was necessary to meet the final constraints.

**Table 2. Initial Parameter Estimates ($\mathbf{X}_0$) and $\Delta$V Magnitudes - Case 1**

| Burn # | Ignition (days) | $\Delta V_x$ (m/s) | $\Delta V_y$ (m/s) | $\Delta V_z$ (m/s) | $\lvert\Delta\mathbf{V}\rvert$ (m/s) |
|---|---|---|---|---|---|
| 1 | 27.723 | 4.393 | 0 | 0 | **4.393** |
| 2 | 55.670 | 4.359 | 0 | 0 | **4.359** |
| 3 | 60.078 | −0.736 | −2.133 | −0.123 | **2.260** |
| 4 | 60.118 | −7.958 | 19.652 | 1.047 | **21.228** |

**Table 3. Final Parameter Estimates ($\mathbf{X}_f$) and $\Delta$V Magnitudes - Case 1**

| Burn # | Ignition (days) | $\Delta V_x$ (m/s) | $\Delta V_y$ (m/s) | $\Delta V_z$ (m/s) | $\lvert\Delta\mathbf{V}\rvert$ (m/s) |
|---|---|---|---|---|---|
| 1 | 27.724 | 4.321 | −6.318 | −0.465 | **7.668** |
| 2 | 55.669 | 3.568 | −5.192 | −0.575 | **6.326** |
| 3 | 60.067 | $5.051e^{-5}$ | $-5.807e^{-5}$ | $-1.423e^{-5}$ | $\mathbf{7.826e^{-5}}$ |
| 4 | 60.107 | −7.742 | 10.444 | 0.924 | **13.034** |

This example is now repeated with slightly different initial and final conditions, as listed in Table 4 (Case 2). In this second case, the vehicle starts in a 100 km altitude, circular, 45° inclined orbit. After the 60-day mission, the vehicle must return to a 100 km altitude circular orbit, but now must meet a constraint on the right ascension of the ascending node ($\Omega$) instead of inclination.

**Table 4. Low Lunar Orbit Initial and Final Conditions - Case 2**

| Element | Initial Condition | Final Condition |
|---|---|---|
| $h$ (km) | 100 | 100 |
| $e$ | 0 | 0 |
| $i$ (deg) | 45 | – |
| $\Omega$ (deg) | 0 | 240 |
| $\omega$ (deg) | 0 | – |
| $\nu$ (deg) | 0 | – |

As before, the optimization problem is solved using *fmincon*. The initial and final parameter estimates ($\mathbf{X}_0$ and $\mathbf{X}_f$) and $\Delta$V magnitudes for Case 2 are given in Tables 5 and 6. Semi-major axis altitude, periapse altitude, apoapse altitude, eccentricity, and $\Omega$ using both the standard strategy and parameter optimization for Case 2 are plotted in Figures 9 through 11. Note in this case that the standard strategy dictates seven burns instead of four, and that the optimized burns result in a noticeably different trajectory than the standard strategy burns. This is most apparent in Figures 9 and 10. Using parameter optimization in Case 2 reduces the orbit maintenance $\Delta$V by **32%** from 131.228 m/s to 89.810 m/s.

## EXTENSIBILITY TO COMPLEX MISSIONS

The low-lunar orbit example shows this approach to be effective for missions with simple constraints. It may also benefit missions with more complex constraints such as LRO. The standard strategy, or stationkeeping algorithm chosen for LRO must meet five constraints:

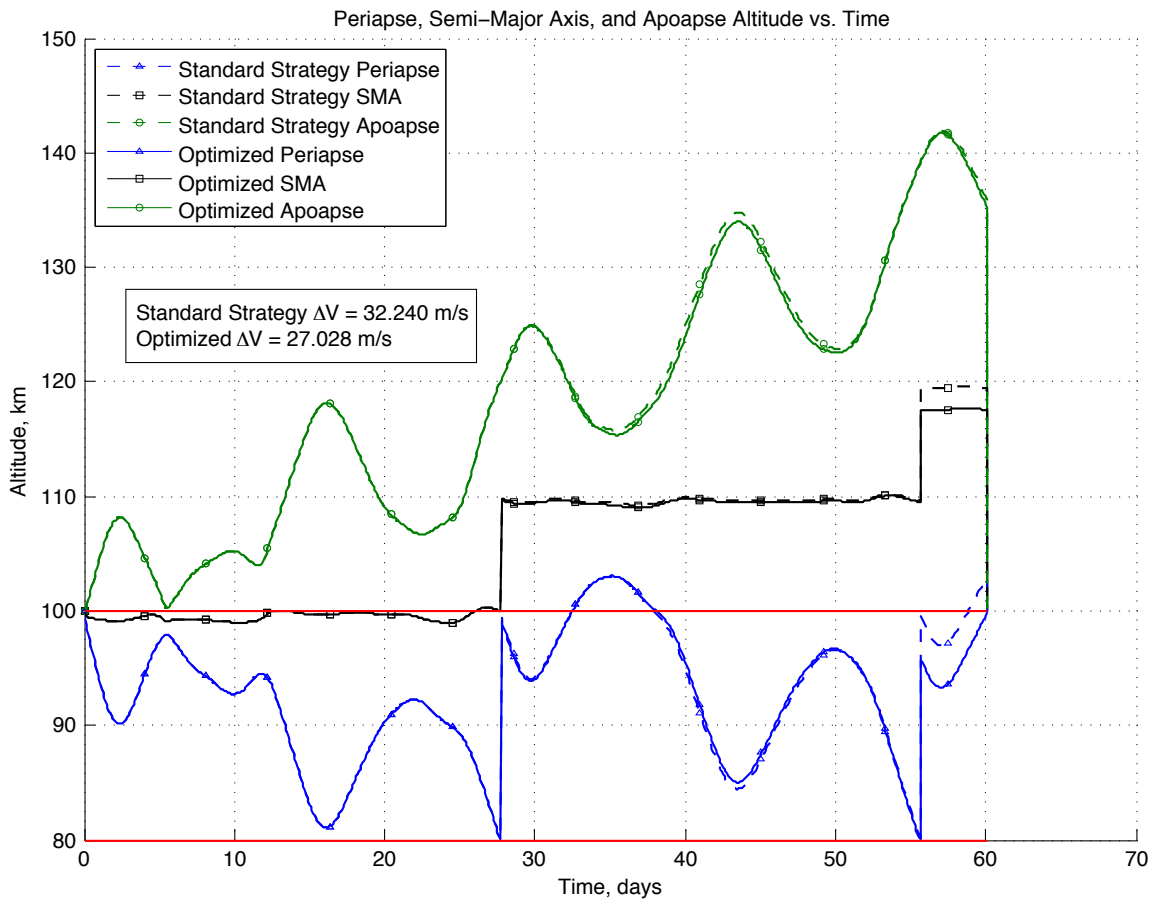


**Figure 6. Periapse, Semi-Major Axis, and Apoapse Altitude vs. Time Using Standard Strategy and Parameter Optimization - Case 1**

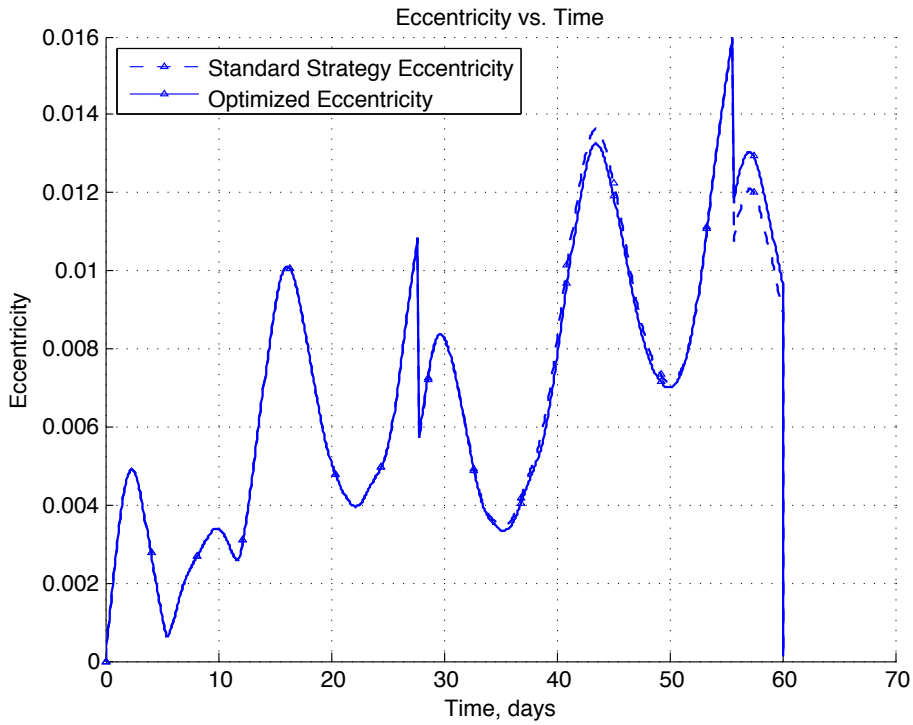


**Figure 7. Eccentricity vs. Time Using Standard Strategy and Parameter Optimization - Case 1**

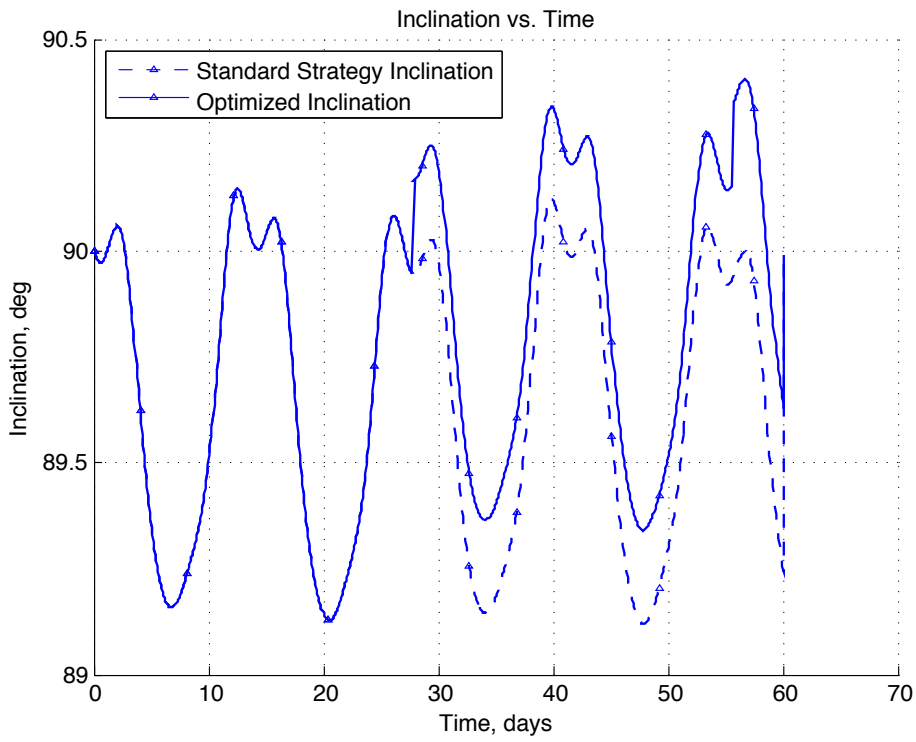


**Figure 8. Inclination vs. Time Using Standard Strategy and Parameter Optimization - Case 1**

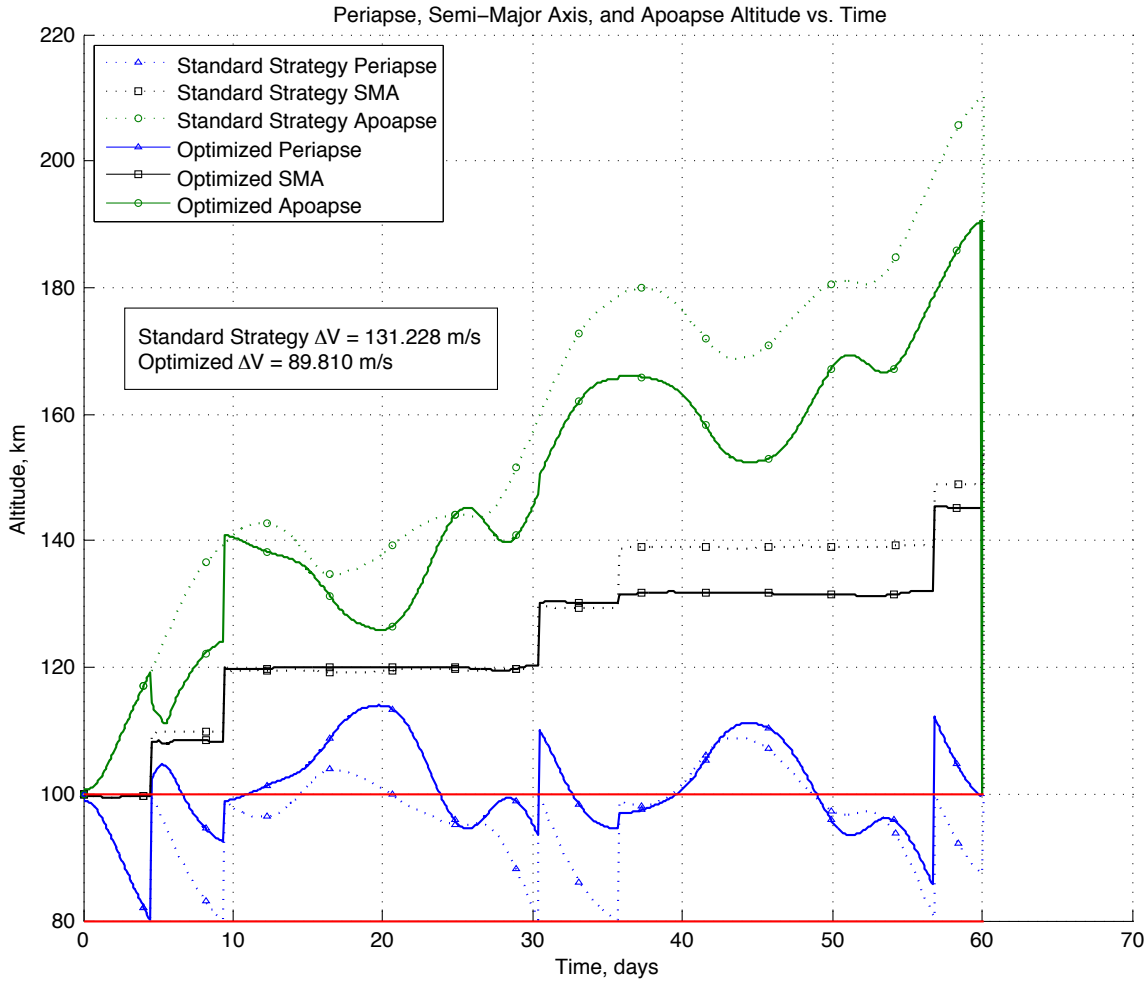


**Figure 9. Periapse, Semi-Major Axis, and Apoapse Altitude vs. Time Using Standard Strategy and Parameter Optimization - Case 2**

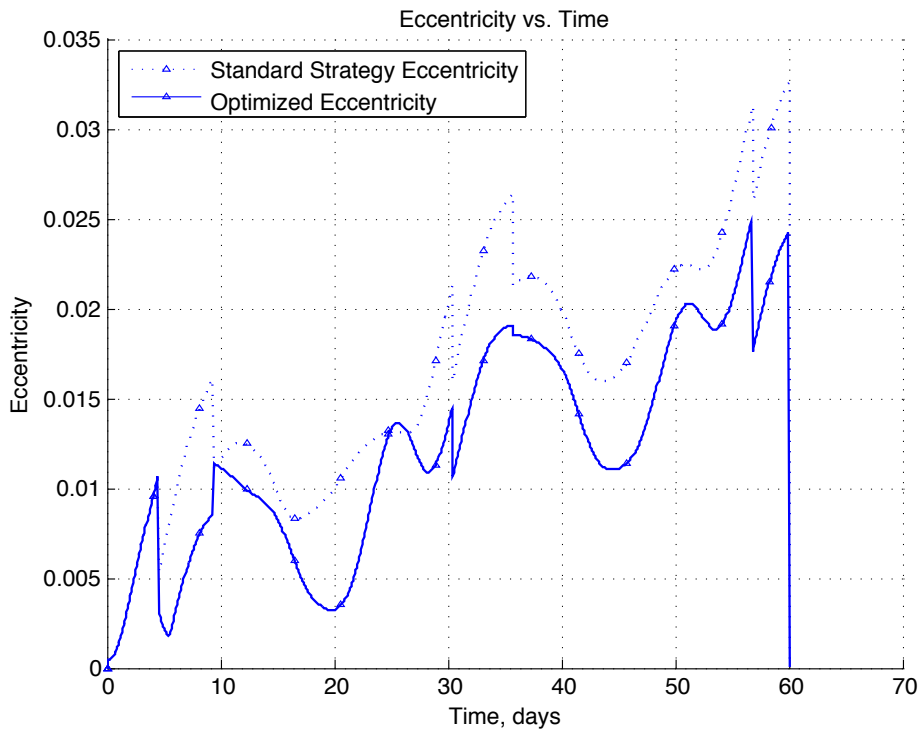


**Figure 10. Eccentricity vs. Time Using Standard Strategy and Parameter Optimization - Case 2**

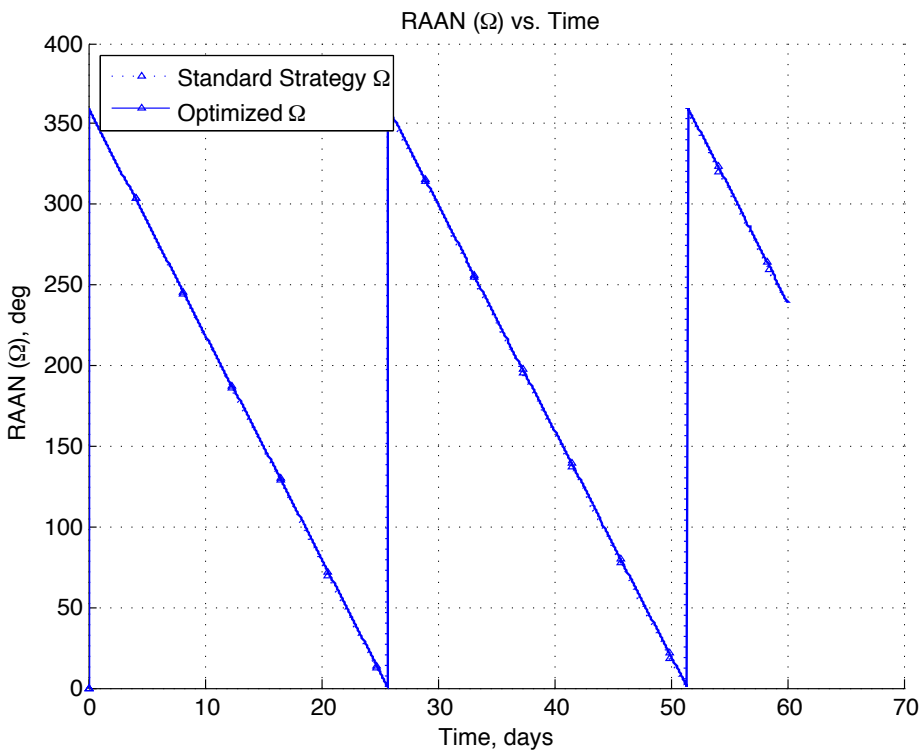


**Figure 11. Inclination vs. Time Using Standard Strategy and Parameter Optimization - Case 2**

**Table 5. Initial Parameter Estimates ($\mathbf{X}_0$) and $\Delta$V Magnitudes - Case 2**

| Burn # | Ignition (days) | $\Delta V_x$ (m/s) | $\Delta V_y$ (m/s) | $\Delta V_z$ (m/s) | $\lvert\Delta\mathbf{V}\rvert$ (m/s) |
|---|---|---|---|---|---|
| 1 | 4.492 | 4.493 | 0 | 0 | **4.493** |
| 2 | 9.361 | 4.247 | 0 | 0 | **4.247** |
| 3 | 30.378 | 4.446 | 0 | 0 | **4.446** |
| 4 | 35.738 | 4.195 | 0 | 0 | **4.195** |
| 5 | 56.835 | 4.420 | 0 | 0 | **4.420** |
| 6 | 60.085 | 0.583 | −84.592 | −4.103 | **84.694** |
| 7 | 60.110 | −23.607 | 7.126 | 1.918 | **24.734** |

**Table 6. Final Parameter Estimates ($\mathbf{X}_f$) and $\Delta$V Magnitudes - Case 2**

| Burn # | Ignition (days) | $\Delta V_x$ (m/s) | $\Delta V_y$ (m/s) | $\Delta V_z$ (m/s) | $\lvert\Delta\mathbf{V}\rvert$ (m/s) |
|---|---|---|---|---|---|
| 1 | 4.508 | 3.532 | −36.650 | −21.799 | **42.789** |
| 2 | 9.334 | 5.105 | 8.562 | 5.415 | **11.344** |
| 3 | 30.388 | 4.449 | −1.942 | −1.029 | **4.962** |
| 4 | 35.746 | 0.648 | −0.006 | 0.026 | **0.648** |
| 5 | 56.736 | 5.933 | −4.359 | −1.916 | **7.608** |
| 6 | 60.000 | −1.001 | 0.527 | 0.229 | **1.154** |
| 7 | 60.000 | −18.477 | 9.828 | 3.990 | **21.305** |

1. Maintain ground station contact during stationkeeping maneuvers.

2. Control altitude to within 20 km of the mean 50 km altitude.

3. Control periselene to spend at least 48% of the time in each of the northern and southern hemispheres.

4. Match orbit eccentricity at the beginning and the end of each lunar siderial period.

5. Minimize stationkeeping $\Delta$V.

In the analysis for LRO, four different stationkeeping options were proposed that meet the first four constraints. Two of the options were eliminated by the fifth constraint, with the remaining two having nearly identical $\Delta$V costs. The option with the smaller altitude variation during each siderial period was chosen as the final stationkeeping algorithm. When simulated, the vehicle coasts through a full siderial period, and then performs a pair of stationkeeping maneuvers to rotate the line of apsides and reset the eccentricity ($e$) vs. argument of periapse ($\omega$) pattern. 10.81 m/s of $\Delta$V per siderial period are required for the stationkeeping maneuvers.

Though a detailed analysis is not addressed in this paper, the mapping from the simple low-lunar orbit mission to the more complex LRO mission is clear. The stationkeeping algorithm chosen for LRO can be used to determine the burns needed over the course of the mission, which then form the initial estimate of the burn parameters. The burns can then be optimized to reduce stationkeeping $\Delta$V, subject to the first four LRO constraints.

## APPROACH LIMITATIONS

While burn parameter optimization can be used to reduce orbit maintenance $\Delta$V, there are limitations to this approach. First, employing an SQP algorithm or other line-search technique will yield only *locally* optimal solutions. The solutions will be local to the initial estimate of the burn parameters, which in this case is defined by the standard strategy. These solutions may or may not be globally optimal, which can only be determined using global optimization techniques such as genetic algorithms. Such analysis is beyond the scope of this paper.

Second, the standard strategy itself represents only one approach to generating an initial estimate. Myriad other equally valid approaches exist, such as performing smaller but more frequent burns throughout the mission. A related variant would be to choose a different and potentially time-varying reference altitude for the periapse-raising burns. Finally, burns could be executed based on other criteria, and not solely on violations of the minimum altitude threshold. A separate analysis (also beyond the scope of this paper) would be required to determine the best (or at least a better) approach to generating an initial estimate.

Third, this approach works well as long as the total number of burns is relatively small. Each time a new burn added, the parameter set grows by four $(t,\ \Delta\mathbf{V}_x,\ \Delta\mathbf{V}_y,\ \Delta\mathbf{V}_z)$, and finite difference gradient computations become more expensive. In Case 1 of the low-lunar orbit example, the gradient of **c** is a (16 x 7) matrix (16 parameters, 4 path inequality constraints, and 3 endpoint equality constraints) and is relatively inexpensive to evaluate. If there were, say, 50 burns, the gradient matrix would be (200 x 53) (200 parameters, 50 path inequality constraints, and 3 endpoint equality constraints), and would be more expensive to evaluate.

## CONCLUSIONS

This study presented a strategy for obtaining a minimum $\Delta$V solution to the orbit maintenance problem using burn parameter optimization. This strategy is well-suited for low-altitude missions in particular given their potentially high $\Delta$V costs for orbit maintenance. Two variations of a low-lunar orbit example were analyzed using this strategy. Orbit maintenance $\Delta$V was reduced by 16% in the first case, and 32% in the second case over using a standard strategy alone.

The general approach for a given mission is to use a pre-existing orbit maintenance strategy to generate an initial estimate of the burn parameters and a baseline $\Delta$V cost. The burn parameters (**X**) are then fed into a parameter optimization algorithm that varies **X** to minimize the total orbit maintenance $\Delta$V while meeting mission constraints. Upon convergence, the final estimate of the burn parameters provides at least a locally optimal solution to the orbit maintenance problem.

Though not analyzed here, in principle this approach can be applied to more complex missions such as LRO. It is not without limitations however, as the standard strategy provides only one approach to generating an initial estimate of the burn parameters. Furthermore, as the number of burns to be optimized increases, the approach becomes more computationally expensive.

## ACKNOWLEDGEMENTS

The author would like to thank Dr. Greg Holt at the NASA Johnson Space Center for his technical review of this paper.

## REFERENCES


[1] B. M. McDonald and S. B. Teplitz, "Space Station Freedom Altitude Strategy," *Flight Mechanics/Estimation Theory Symposium*, Greenbelt, MD, May 1990.

[2] R. S. Bhat, B. E. Shapiro, R. B. Frauenholz, and R. K. Leavitt, "TOPEX/Poseidon Orbit Maintenance for the First Five Years," *AAS/GSFC International Symposium on Space Flight Dynamics*, Greenbelt, MD, May 1998. AAS 98-379.

[3] M. Beckman and R. Lamb, "Stationkeeping for the Lunar Reconnaissance Orbiter," *20th International Symposium on Space Flight Dynamics*, Annapolis, MD, September 2007.

[4] A. L. Bowes *et al.*, "Primary Science Orbit Design for the Mars Reconnaissance Orbiter Mission," *AAS/AIAA Space Flight Mechanics Conference*, Ponce, Puerto Rico, February 2003. AAS 03-212.

[5] C. A. Ocampo, "The Optimization of Orbital Paths," DRAFT, March 2009.

[6] C. H. Westhelle, "Lunar Orbit Altitude Maintenance Study," Final Report EG-CEV-06-26, NASA Johnson Space Center, Engineering Directorate, Houston, TX, April 2006.

[7] D. R. Adamo, "A Precision Orbit Predictor Optimized For Complex Trajectory Operations," *AAS/AIAA Astrodynamics Specialists Conference*, Big Sky, MT, August 2003. AAS 03-665.

[8] J. Nocedal and S. J. Wright, *Numerical Optimization*. Springer Series in Operations Research, Springer Verlag, 2nd ed., 2006.

# A Minimum ΔV Orbit Maintenance Strategy for Low-Altitude Missions Using Burn Parameter Optimization

Aaron J. Brown

*NASA Johnson Space Center*

August 4, 2011

# Introduction

- Orbit Maintenance is the series of burns performed during a mission to ensure the orbit satisfies mission constraints.
- Low-altitude missions often need non-trivial orbit maintenance ΔV due to perturbations and minimum-altitude thresholds.
- Goal is to minimize orbit maintenance ΔV using burn parameter optimization

# The Big (Abstract) Picture

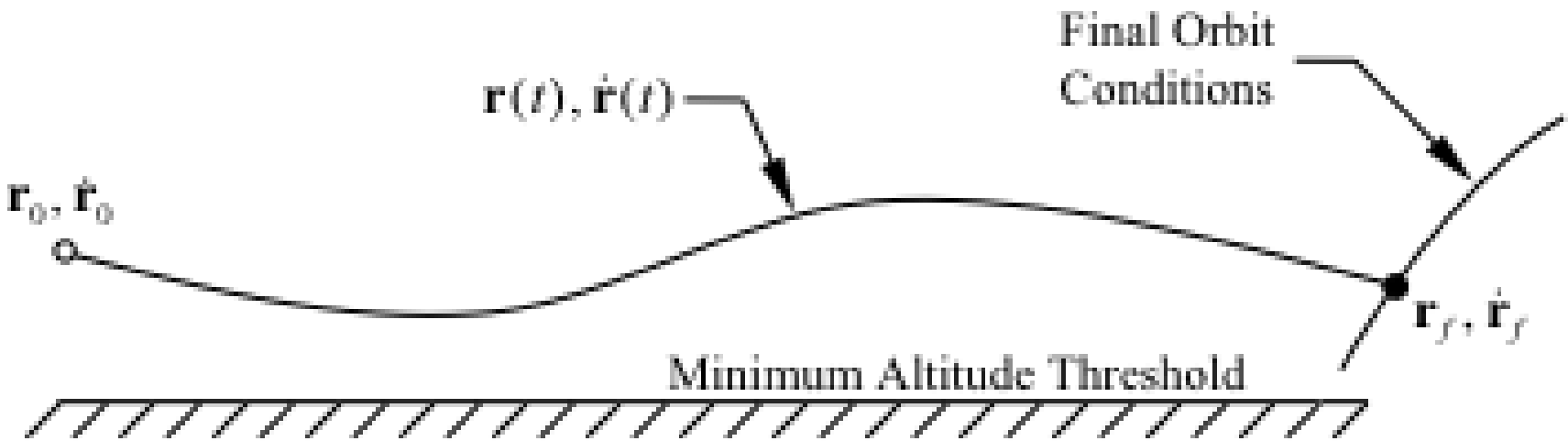

# Standard Strategy – Part I

- Use a standard orbit maintenance strategy to define burn parameters and generate initial estimates.
- Propagate until periapse drops below the minimum altitude.
- Perform a horizontal burn at the prior apoapse in order to raise periapse.
- Repeat as necessary over the course of the mission.

# Standard Strategy – Part II

- Periapse-raising alone will not meet final orbit conditions.

- After periapse-raising phase, perform a separate, minimum ΔV two-burn impulsive transfer to meet final conditions.

# Example: Low Lunar Orbit – Case 1

**Table 1. Low Lunar Orbit Initial and Final Conditions - Case 1**

| Element | Initial Condition | Final Condition |
|---|---|---|
| $h$ (km) | 100 | 100 |
| $e$ | 0 | 0 |
| $i$ (deg) | 90 | 90 |
| $\Omega$ (deg) | 0 | – |
| $\omega$ (deg) | 0 | – |
| $\nu$ (deg) | 0 | – |

- Minimum altitude = 80 km
- 60-day mission

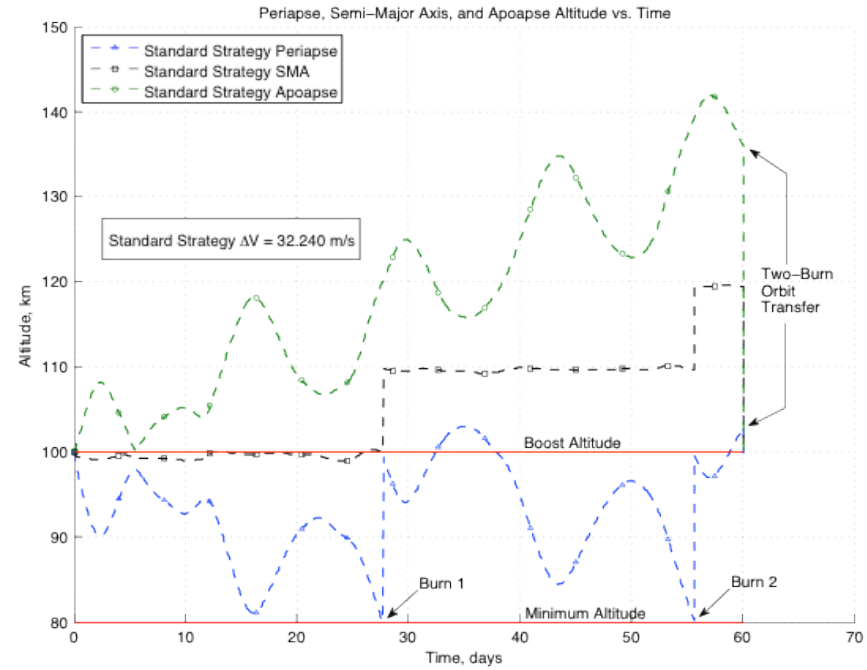


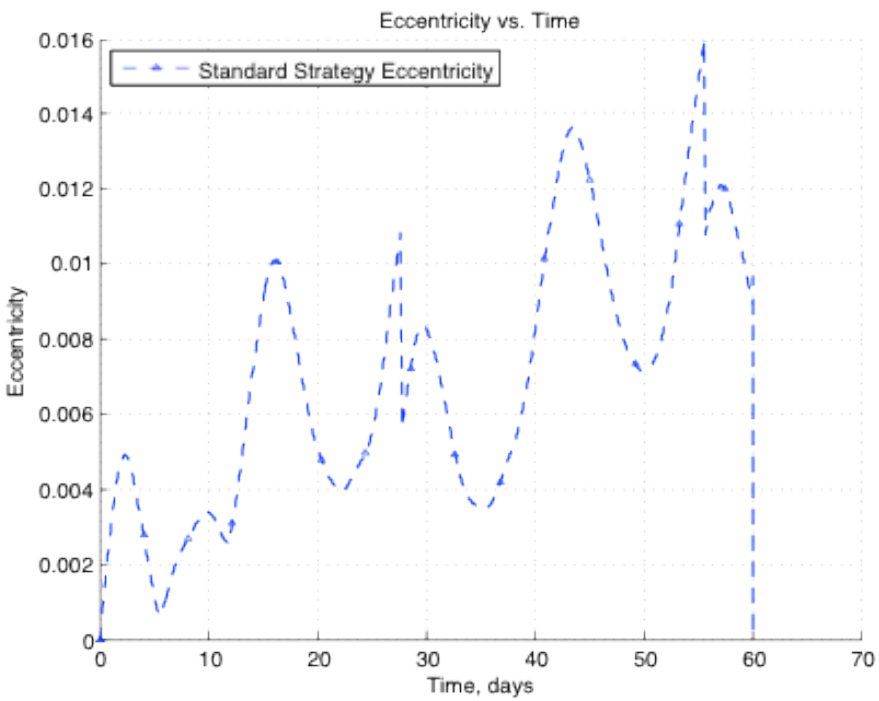


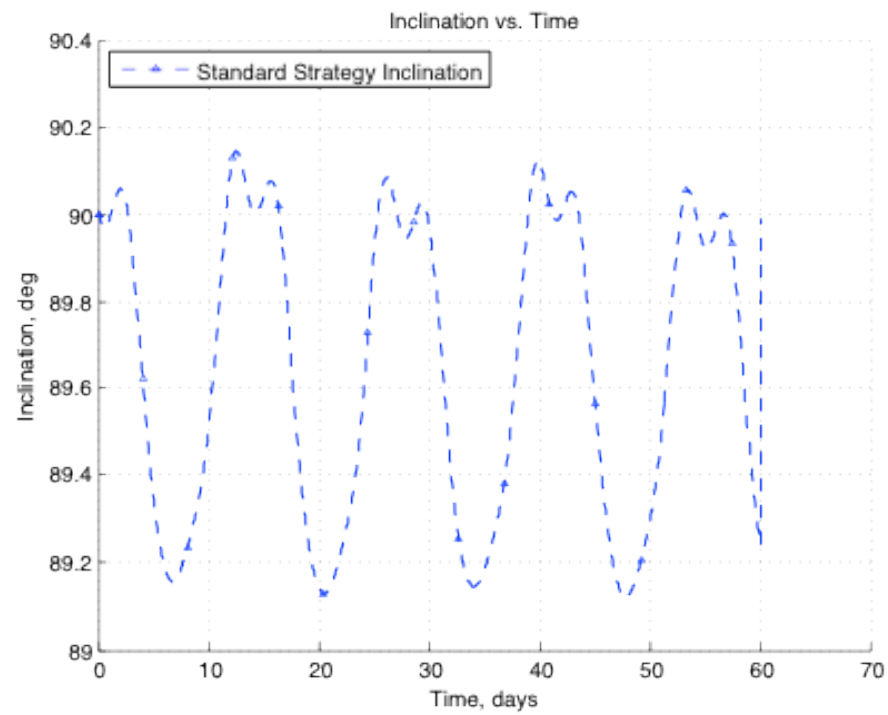

# Parameter Optimization

- Standard strategy is not only feasible, but potentially optimal on its own.
- But…we can do better using parameter optimization.
- Use ignition times and ΔV components of all standard strategy burns as parameters (**X**) for the main optimization problem.

# Problem Statement

Minimize

$$J(\mathbf{X}) = \sum_{k=1}^{N} \Delta \mathrm{V}_k$$

Subject to

$$\mathbf{c}_{eq}(\mathbf{r}_f, \dot{\mathbf{r}}_f) = \mathbf{0}$$

$$h(t) \geq h_{\min}$$

- $\mathbf{X} = \begin{pmatrix} t_1 & \Delta\mathbf{V}_1 & t_2 & \Delta\mathbf{V}_2 & \cdots & t_N & \Delta\mathbf{V}_N \end{pmatrix}$
- $N$ is the number of impulsive burns
- $t_0, t_f, \mathbf{r}_0, \dot{\mathbf{r}}_0$ are specified

# Problem Statement, cont.

- Convert minimum altitude path constraint to point constraint at periapse prior to each burn.

$$h(t) \geq h_{\min} \quad \text{becomes} \quad \mathbf{c}_{ineq} = \begin{pmatrix} h_{\min} - h_{p_1} \\ h_{\min} - h_{p_2} \\ \vdots \\ h_{\min} - h_{p_N} \end{pmatrix} \leq \mathbf{0}.$$

# Problem Statement, cont.

- Gradient of *J* is straight-forward

$$\left(\frac{\partial J}{\partial \mathbf{X}}\right) = \begin{pmatrix} 0 & \frac{\Delta \mathbf{V}_1^{\mathrm{T}}}{\Delta \mathrm{V}_1} & 0 & \frac{\Delta \mathbf{V}_1^{\mathrm{T}}}{\Delta \mathrm{V}_1} & \mathrm{L} & 0 & \frac{\Delta \mathbf{V}_N^{\mathrm{T}}}{\Delta \mathrm{V}_N} \end{pmatrix}$$

- Gradients of $\mathbf{c}_{eq}$ and $\mathbf{c}_{ineq}$ must be approximated (finite differences, etc.)

# Solution and Results – Case 1

- Using parameter optimization reduced orbit maintenance ΔV from 32.240 m/s to 27.028 m/s -- a 16% savings over using the standard strategy alone.

**Table 2. Initial Parameter Estimates ($\mathbf{X}_0$) and $\Delta$V Magnitudes - Case 1**

| Burn # | Ignition (days) | $\Delta V_x$ (m/s) | $\Delta V_y$ (m/s) | $\Delta V_z$ (m/s) | $\lvert\Delta V\rvert$ (m/s) |
|---|---|---|---|---|---|
| 1 | 27.723 | 4.393 | 0 | 0 | **4.393** |
| 2 | 55.670 | 4.359 | 0 | 0 | **4.359** |
| 3 | 60.078 | −0.736 | −2.133 | −0.123 | **2.260** |
| 4 | 60.118 | −7.958 | 19.652 | 1.047 | **21.228** |

**Table 3. Final Parameter Estimates ($\mathbf{X}_f$) and $\Delta$V Magnitudes - Case 1**

| Burn # | Ignition (days) | $\Delta V_x$ (m/s) | $\Delta V_y$ (m/s) | $\Delta V_z$ (m/s) | $\lvert\Delta V\rvert$ (m/s) |
|---|---|---|---|---|---|
| 1 | 27.724 | 4.321 | −6.318 | −0.465 | **7.668** |
| 2 | 55.669 | 3.568 | −5.192 | −0.575 | **6.326** |
| 3 | 60.067 | $5.051e^{-5}$ | $-5.807e^{-5}$ | $-1.423e^{-5}$ | $\mathbf{7.826e^{-5}}$ |
| 4 | 60.107 | −7.742 | 10.444 | 0.924 | **13.034** |

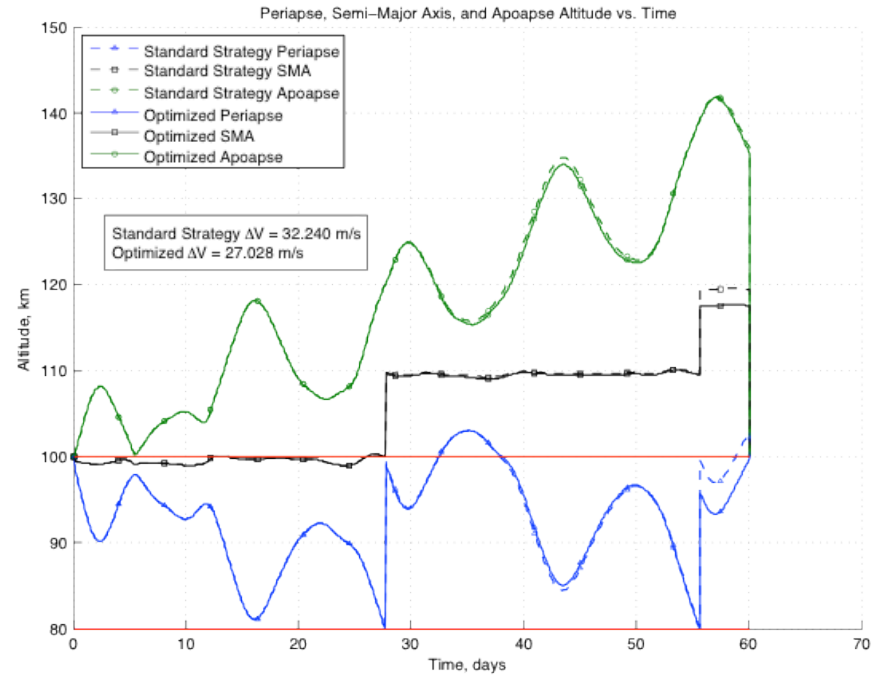


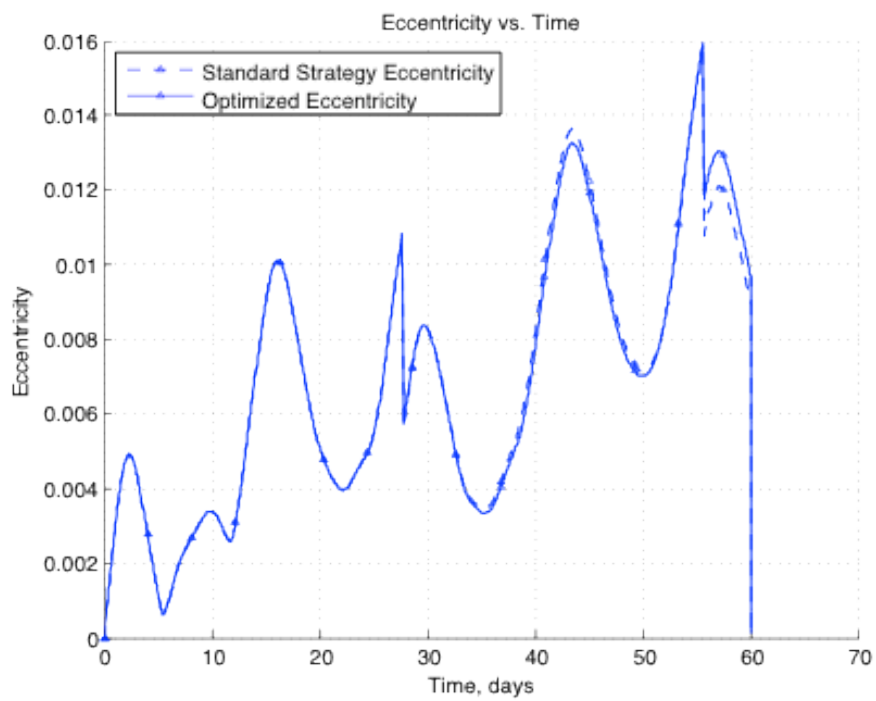


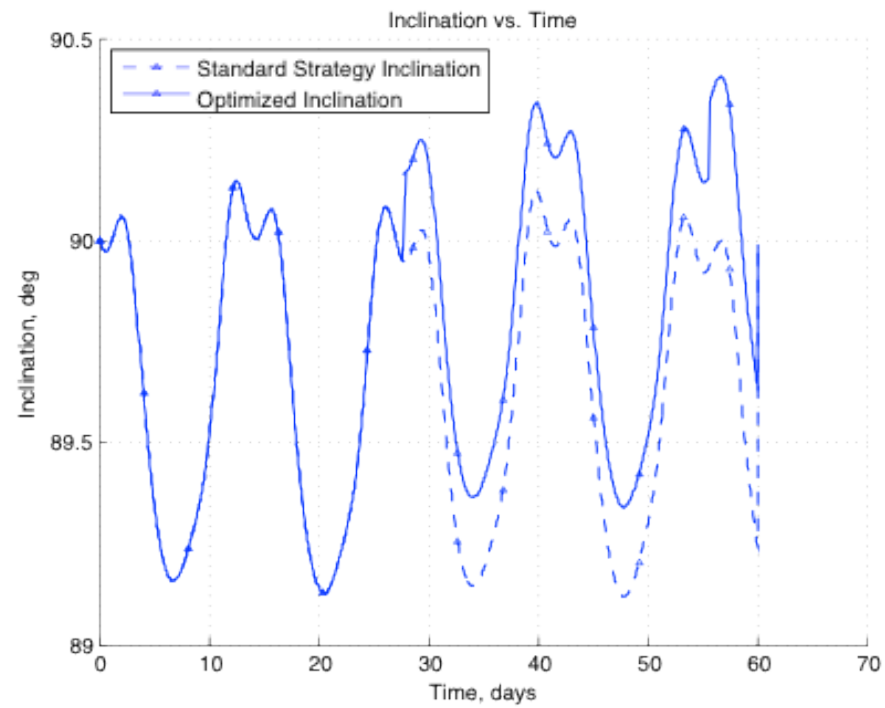

# Example: Low Lunar Orbit – Case 2

**Table 4. Low Lunar Orbit Initial and Final Conditions - Case 2**

| Element | Initial Condition | Final Condition |
|---|---|---|
| $h$ (km) | 100 | 100 |
| $e$ | 0 | 0 |
| $i$ (deg) | 45 | – |
| $\Omega$ (deg) | 0 | 240 |
| $\omega$ (deg) | 0 | – |
| $\nu$ (deg) | 0 | – |

- Minimum altitude = 80 km
- 60-day mission

# Solution and Results – Case 2

- Using parameter optimization reduced orbit maintenance ΔV from 131.228 m/s to 89.810 m/s -- a 32% savings over using the standard strategy alone.

**Table 2. Initial Parameter Estimates ($\mathbf{X}_0$) and $\Delta$V Magnitudes - Case 1**

| Burn # | Ignition (days) | $\Delta V_x$ (m/s) | $\Delta V_y$ (m/s) | $\Delta V_z$ (m/s) | $\lvert\Delta V\rvert$ (m/s) |
|---|---|---|---|---|---|
| 1 | 27.723 | 4.393 | 0 | 0 | **4.393** |
| 2 | 55.670 | 4.359 | 0 | 0 | **4.359** |
| 3 | 60.078 | −0.736 | −2.133 | −0.123 | **2.260** |
| 4 | 60.118 | −7.958 | 19.652 | 1.047 | **21.228** |

**Table 3. Final Parameter Estimates ($\mathbf{X}_f$) and $\Delta$V Magnitudes - Case 1**
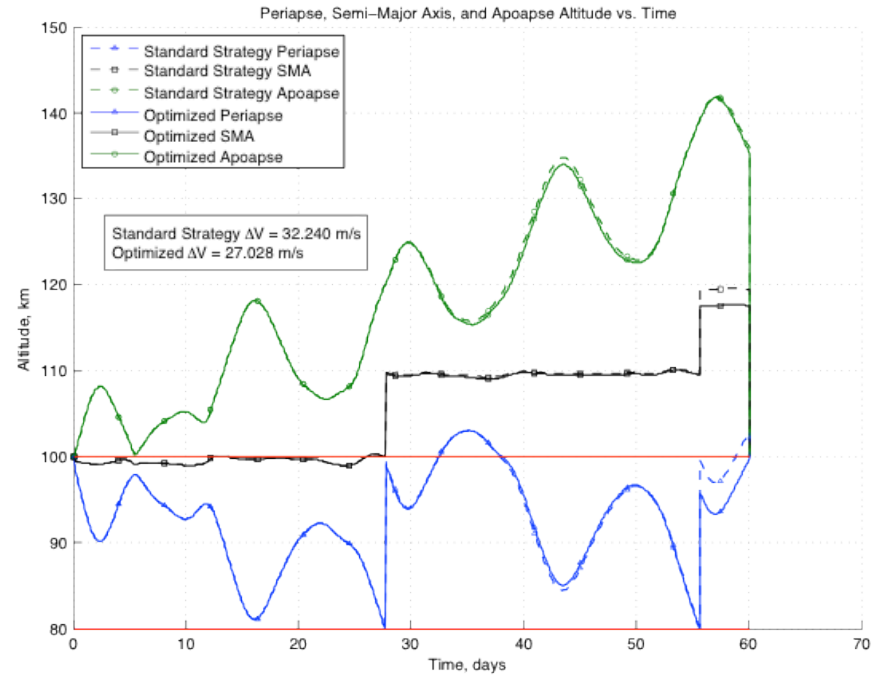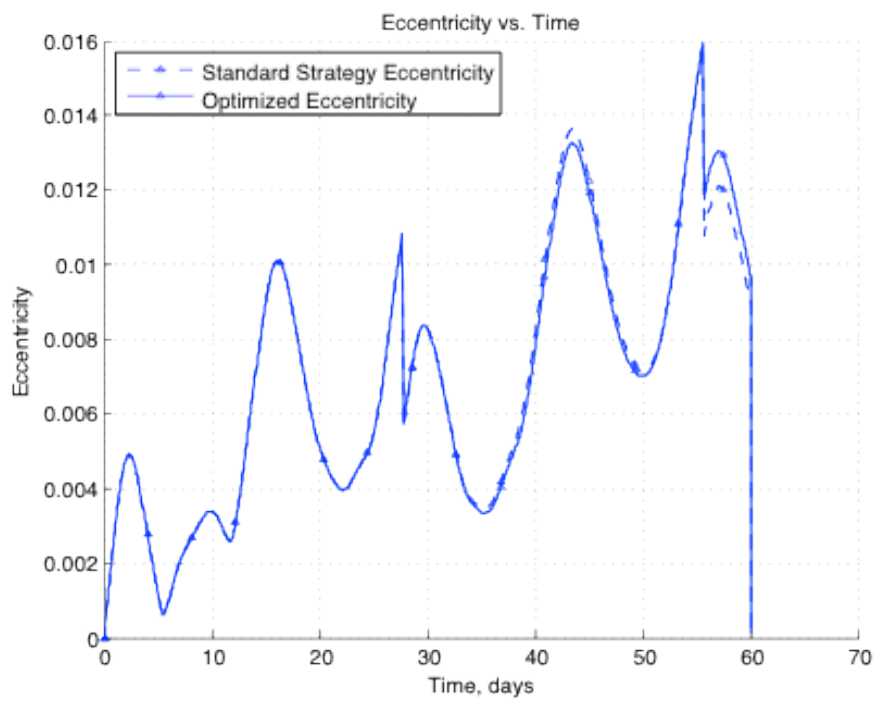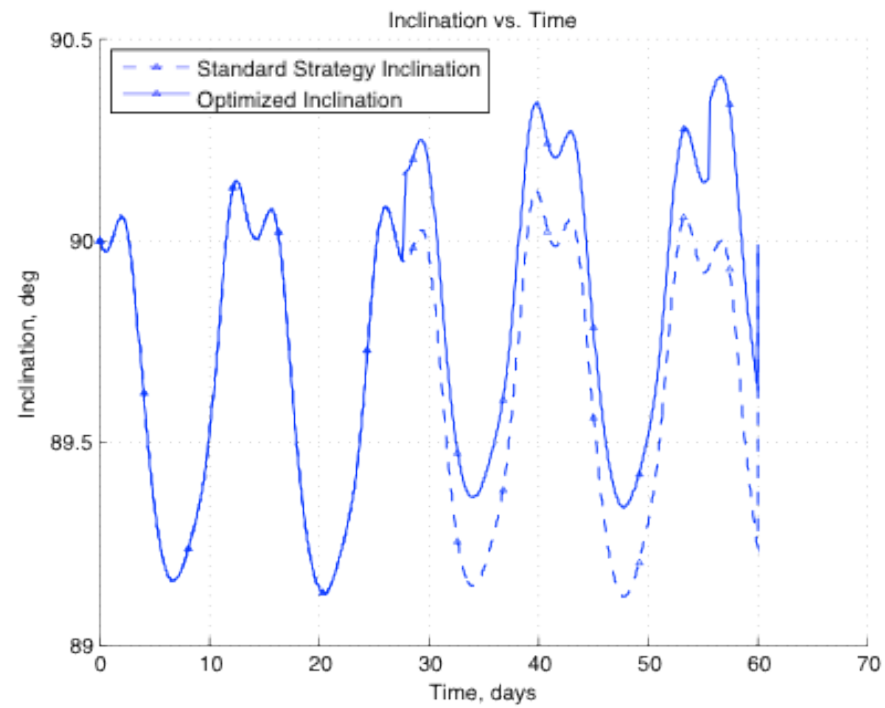
| Burn # | Ignition (days) | $\Delta V_x$ (m/s) | $\Delta V_y$ (m/s) | $\Delta V_z$ (m/s) | $\lvert\Delta V\rvert$ (m/s) |
|---|---|---|---|---|---|
| 1 | 27.724 | 4.321 | −6.318 | −0.465 | **7.668** |
| 2 | 55.669 | 3.568 | −5.192 | −0.575 | **6.326** |
| 3 | 60.067 | $5.051e^{-5}$ | $-5.807e^{-5}$ | $-1.423e^{-5}$ | $\mathbf{7.826e^{-5}}$ |
| 4 | 60.107 | −7.742 | 10.444 | 0.924 | **13.034** |